J Nanostruct 15(4): 2293-2302, Autumn 2025

RESEARCH PAPER

$YbFeTi_2O_7$ Nanoparticles as Magnetically Separable Photocatalyst for Degradation of Methylene Blue under Visible Light Irradiation

Sadeq Khudhur Thajeel [1], Luay Mannaa Ibrahim [2], Ghassan Jasim Hadi [2], Mohamed Ahmed [3], Qais R. Lahhob [4]*, Mustafa Mudhafar [5,6]

[1] *College of Technical Engineering, National University of Science and Technology, Dhi Qar, Iraq*

[2] *College of Health and Medical Techniques, Northern Technical University, Al-Dour, Iraq*

[3] *Department of Physics, College of Science, University of Sumer, Iraq*

[4] *Collage of Pharmacy, National University of Science and Technology, Dhi Qar, 64001, Iraq*

[5] *Department of Anesthesia Techniques and Intensive Care, Al-Taff university College, 56001, Kerbala, Iraq*

[6] *Department of Chemistry, Faculty of Science and Mathematics, Universiti Pendidikan Sultan Idris, Proton City, Perak, Tanjung Malim, 35900, Malaysia*

ARTICLE INFO

Article History:
Received 05 June 2025
Accepted 27 September 2025
Published 01 October 2025

Keywords:
Magnetically separable
Methylene blue
Photocatalyst
Visible light
$YbFeTi_2O_7$ nanoparticles

ABSTRACT

$YbFeTi_2O_7$ nanoparticles (YFTO) were synthesized by the sol-gel method. The nanoparticles exhibited superior photocatalytic activity under visible light irradiation, confirmed by diffuse reflectance spectroscopy (DRS). Enhanced visible light absorption along with a proper band gap value of 2.44 eV validated the potential of synthesized nanoparticles as the visible light photocatalyst. Methylene blue (MB) aqueous solution was chosen as an organic pollutant to investigate the photocatalytic efficiency of the YFTO nanoparticles. After 120 min illumination under visible light, more than 95% of the MB solution was degraded using 0.03 g of the YFTO nanoparticles. Some of the important determinants, including amount of photocatalyst and pH of MB solution, were considered to find the optimal conditions for photoactivity of the YFTO nanoparticles. Due to demonstrating the superparamagnetic property, the YFTO nanoparticles offered the ease of recovery which is crucial to provide significant reusability. In this regard, the magnetically separable YFTO showed great reusability over 5 consecutive reaction cycles. The photodegradation mechanism was studied using different radical scavenger agents, showing that hydroxyl (•OH) and superoxide ($\bullet O_2^-$) radicals involved in the degradation of MB molecules.

How to cite this article
Thajeel S., Ibrahim L, Hadi G., Ahmed M., Lahhob Q., Mudhafar M. $YbFeTi_2O_7$ Nanoparticles as Magnetically Separable Photocatalyst for Degradation of Methylene Blue under Visible Light Irradiation. J Nanostruct, 2025; 15(4):2293-2302. DOI: 10.22052/JNS.2025.04.068

INTRODUCTION

Photocatalysis is an efficient alternative for common treatment techniques, which are unable to remove complex and persistent contaminants from the aqueous media [1, 2]. Annually, millions of tons of organic compound, including surfactants, dyes, pesticides, and oil based chemicals, are discharged into water resources

* *Corresponding Author Email: qaisrlahhob@gmail.com*

as wastes, posing a significant threat to marine ecosystem, and in turn to public health [3]. Recent increase in the water contamination has raised serious concerns, as we humans rely on oceans and rivers to supply food and drinking water. Of the pollutants discharged into the environment, effluent from textile dyeing industries is the big challenge, because of its adverse impacts on the human health. It is well known that organic dyes can cause cancerous diseases or neurological disorders [4, 5].

Although photocatalytic process is the promising approach for the environmental remediation, its large-scale applications restrict by some limitations [6]. Common photocatalysts such as TiO_2 and ZnO have the wide range band gap corresponding to the energy of light in the UV region [7]. This point specifies that the high energy is needed to activate the photocatalysts [8]. Furthermore, rapid recombination rate of charge carriers is strongly decreased the photocatalytic performance [8]. Tailoring the photocatalyst composition has been proposed to surmount these limitations and render the photocatalysts suitable for degradation of wide range of the organic pollutants. In this regard, mixed metal oxides have received considerable attention due to their superior properties in batteries [9], energy production [10], solar cell [10], and photocatalysis [11]. Electronic transition between different energy levels of coupled metal oxide materials effectively minimize electron–hole pair recombination and improve photocatalytic activity in the visible light range [8, 12]. For instance, Abed et. al synthesized $CuEr_2TiO_6$ nanoparticles by sol-gel Pechini and studied their photocatalytic activity for degradation of acid red 88 under visible light irradiation [13]. Also, photocatalytic activity of $CoFe_2O_4/Bi_2MoO_6$ was studied for degradation of rhodamine blue under visible light irradiation [14].

Besides, reusability of photocatalysts is crucial to for their effective use in the removal of pollutants [15]. Hindering the loss of photocatalysts during the successive uses not only reduces the cost of the photocatalytic utilization, but also minimizes the possible side effects caused by the accumulation of photocatalysts in the environment [16]. To meet this demand, magnetic photocatalysts are the great solution, providing the ease of recovery and reuse of photocatalysts [17, 18].

Herein, efficient and magnetically separable visible-light photocatalyst nanoparticles, $YbFeTi_2O_7$, were prepared using straightforward sol-gel reaction. Characterization of the nanoparticles was performed using XRD, FTIR, FESEM, TEM, VSM, and DRS analyses. To evaluate to the photocatalytic activity of the synthesized nanoparticles, the degradation of an aqueous solution of methylene blue (MB) was studied under the visible light irradiation. Effect of different determinants including pH of MB solution and dosage of the prepared photocatalyst were assessed on the photocatalytic efficiency of the MB degradation.

MATERIALS AND METHODS

Synthesis of photocatalyst

The sol-gel synthetic route was employed to prepare the $YbFeTi_2O_7$ (YFTO) nanoparticles. Initially, 0.02 mmol of citric acid was added to 50 mL of absolute ethanol as a complexing agent, then 2.0 mmol of tetra butyl orthotitanate (TBOT), 1.0 mmol of $Fe(NO_3)_3.9H_2O$, and 1.0 mmol of $Yb(NO_3)_3.5H_2O$ were respectively added under vigorous stirring. After 2 hours of stirring, the obtained sol solution was heated overnight in an oven at 80 °C to form the dried gel. Finally, the dried gel was heated at 600 °C for 6 hours to obtain light brown nanoparticles.

Photocatalytic experiments

The methylene blue (MB) degradation was studied using the synthesized YFTO photocatalyst under the visible light irradiation. For that, 50 mL of MB solution (50 ppm) was illuminated from the distance of 30 cm by an LED lamp (daylight white, 50 W) in the presence of different dosages of the YFTO nanoparticles (0.01, 0.03, 0.05, and 0.07 g). Also, the photocatalytic degradation was investigates using different pH (3, 5, 7, 9, and 11) of MB solution.

The dye solution was first allowed to interact with the photocatalyst particles until adsorption–desorption equilibrium was achieved before illumination. So that the MB solution containing the YFTO photocatalyst was stirred in darkness for 30 min. After that, the degradation level was monitored in constant interval time (30 min) using UV/Vis spectrophotometer at maximum wavelength of MB (668 nm).

Characterization

Crystalline phase of the synthesized YFTO nanoparticles was studied using X-ray diffraction

(XRD) pattern by Philips diffractometer (X'pert Pro MPD, Cu *Kα* = 1.54 Å). Functional groups on the surface of the synthesized YFTO nanoparticles were detected using Fourier transform infrared (FTIR) spectroscopy by Bruker Tensor 27 FTIR spectrophotometer. Morphology of the YFTO nanoparticles was studied using field emission electron microscope (FESEM) (TESCAN mira 3) and transmission electron microscope (TEM) (Zeiss, EM 900). Vibrating sample magnetometer (VSM) (VSM

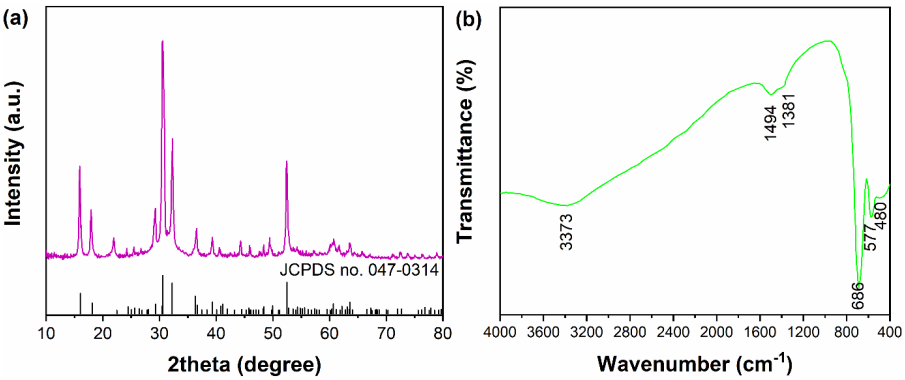

Fig. 1. XRD pattern (a) and FTIR spectrum (b) for the synthesized YFTO nanoparticles.

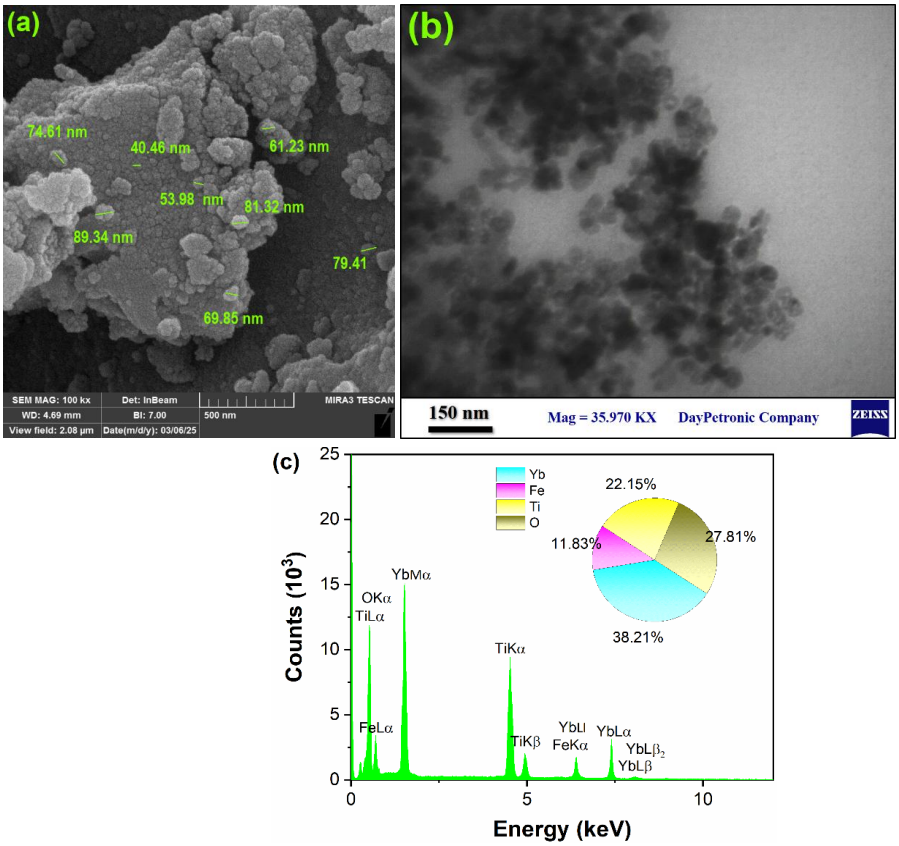

Fig. 2. FESEM (a), TEM (b) images, and EDX spectrum (c) for the YFTO nanoparticles.

MDKB) was used to study the magnetic properties of the YFTO nanoparticles. The diffuse reflectance spectroscopy (DRS) (JASCO UV/Vis V-670) was used to assess the visible-light absorption ability by the nanoparticles.

RESULTS AND DISCUSSION

Structural, morphology, magnetic, and optical investigations

Fig. 1a exhibits the XRD pattern for the synthesized YFTO nanoparticles, confirming all the diffraction planes correspond to the orthorhombic phase of Iron Ytterbium Titanium Oxide (JCPDS file no. 047-0314, space group: Pcnb). The average crystallite size of the synthesized nanoparticles was calculated to be 18.31 nm using Scherrer equation, base on the peak at $2\Theta = 30.5°$.

The FTIR spectrum (Fig. 1b) depicts the functional groups of the YFTO nanoparticles. The broad absorption at around 3400 cm^{-1} is related to the stretching vibration of O-H bonds. The characteristic absorption of metal-oxygen bonds occur at 686 and 577 cm^{-1} which are attributed to the Ti-O and Fe-O respectively [19]. Additionally, the weak peak centered 480 cm^{-1} can be assigned to Yb-O bonds [20]. Two bands at 1490 and 1381 cm^{-1} are assigned to the carbonated group adsorbed on the surface of nanoparticles due to exposing to the ambient condition [21, 22].

The FESEM image in Fig. 2a exhibits the morphology of the YFTO nanoparticles, showing semi-spherical nanoparticles in size range between 40-100 nm. Due to the large surface area of the synthesized nanoparticles, the agglomeration is inevitable, so that larger size nanoparticles are observed in the FESEM image. Moreover, the morphology of the YFTO nanoparticles was studied using TEM image (Fig. 2b), which reveals the semi-spherical nanoparticles with average size below 100 nm. Fig. 2c shows the EDX spectrum of the synthesized YFTO nanoparticles, confirming the existence of constituents of the nanoparticles and success of the synthetic route. Also, inset to the Fig. 2c represents the microanalysis of the YFTO with relative amounts of each components. The M-H curve, shown in Fig. 3, reveals the superparamagnetic behavior for the synthesized YFTO nanoparticles with the saturation magnetization (*Ms*) of 40.95 emu/g. This character assists to recover the photocatalyst nanoparticles from the aqueous media [23]. Using a bar magnet, the YFTO nanoparticles were easily separated from the MB solution. Additionally, due to the zero remnant magnetization in the absence of external magnetic field, the nanoparticles tend to disperse in the MB solution without occurring

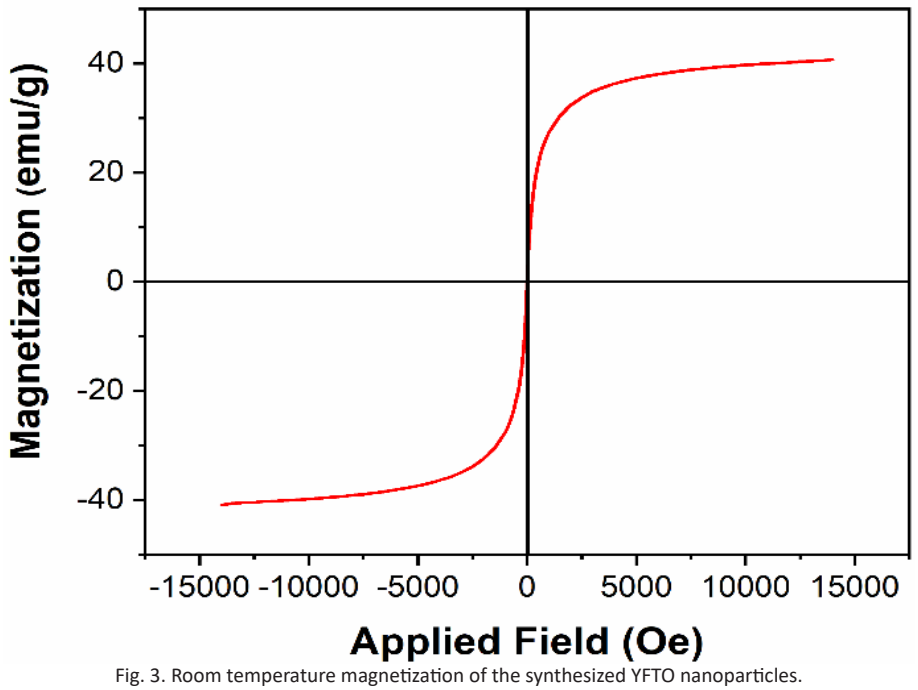

Fig. 3. Room temperature magnetization of the synthesized YFTO nanoparticles.

considerable agglomeration, resulting in the enhanced photocatalytic activity [24].

The optical responses of the synthesized YFTO nanoparticles was investigated by the DRS spectroscopy. The highly promoted visible light absorption is observable in the DRS spectrum (Fig. 4), confirming the potential of the YFTO nanoparticles to serve as the highly activated

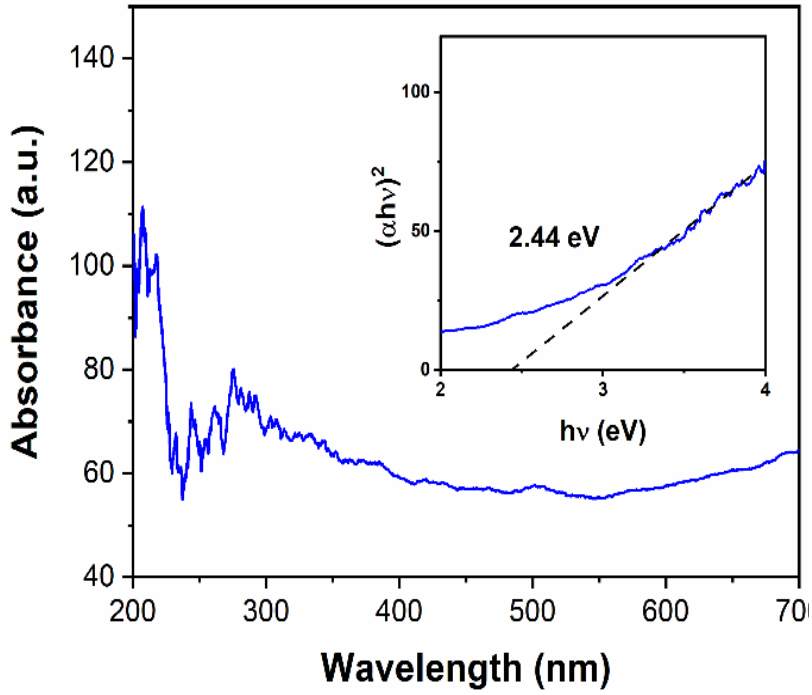

Fig. 4. DRS spectrum of the synthesized YFTO nanoparticles. The inset shows $(\alpha h\nu)^2$ vs. $h\nu$ plot.

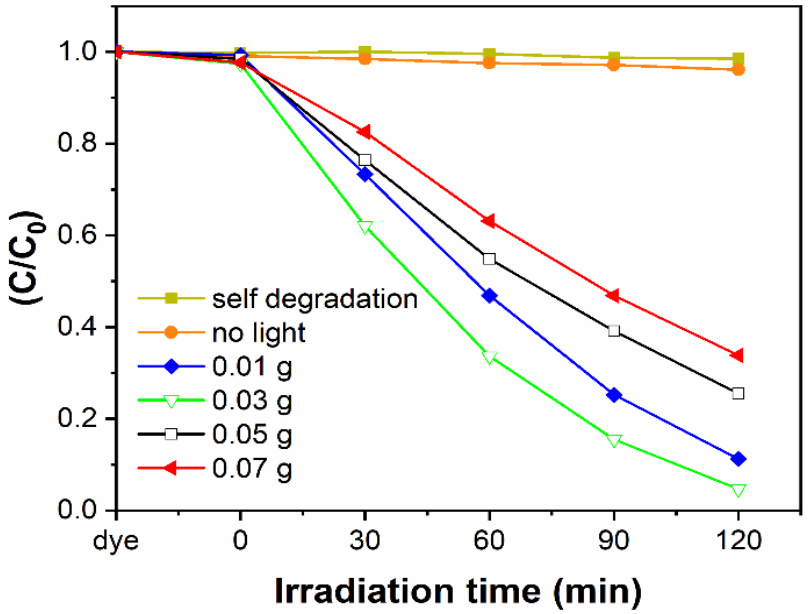

Fig. 5. Photodegradation of MB solution using different amounts of the YFTO nanoparticles.

visible light photocatalyst. This result is truly attributed to the electron transitions between the components, that is, Yb_2O_3, Fe_2O_3, and TiO_2, which substantially increases the visible light sensitivity of the nanoparticles and also decreases the recombination rate of the charge carriers [25-27]. The inset to Fig. 4 shows the determined the band gap of the nanoparticles was calculated by the Tauc method. The optical band gap of the YFTO nanoparticles was determined to be 2.44 eV which corresponds to the energy of photons in the visible light region.

Photocatalytic investigations

Photocatalyst amount

The photocatalytic oxidation of MB solution was studied using different amount of the YFTO nanoparticles (0.01, 0.03, 0.05, and 0.07 g), which is shown in Fig. 5. As can be seen in Fig. 5, the YFTO nanoparticles is able to efficiently degrade the MB molecules under 120 min illumination by the visible light irradiation. The highest degradation performance was 95.32% using 0.03 g of the synthesized YFTO. The exceeded amount of the YFTO nanoparticles led to the significant reduction of the photodegradation efficiency. Because photocatalyst particles require photons with sufficient energy for activation, excessive dispersion of nanoparticles in the turbid dye solution limits light penetration and consequently decreases photocatalytic efficiency [28].

Furthermore, Fig. 5 shows without addition of any the YFTO nanoparticles, the MB solution hardly decomposes on its own when exposed to visible light. Also, under no light condition, the reduction in the MB absorption is insignificant, confirming that the reduced absorption of the MB solution during illumination is attributed to the degradation of the MB molecules nor adsorption on the surface of the nanoparticles.

Effect of pH

The pH of dye solution impacts the surface charges of photocatalyst, thereby affecting the adsorption of dye molecules. Since the photocatalytic reaction primarily occurs on the

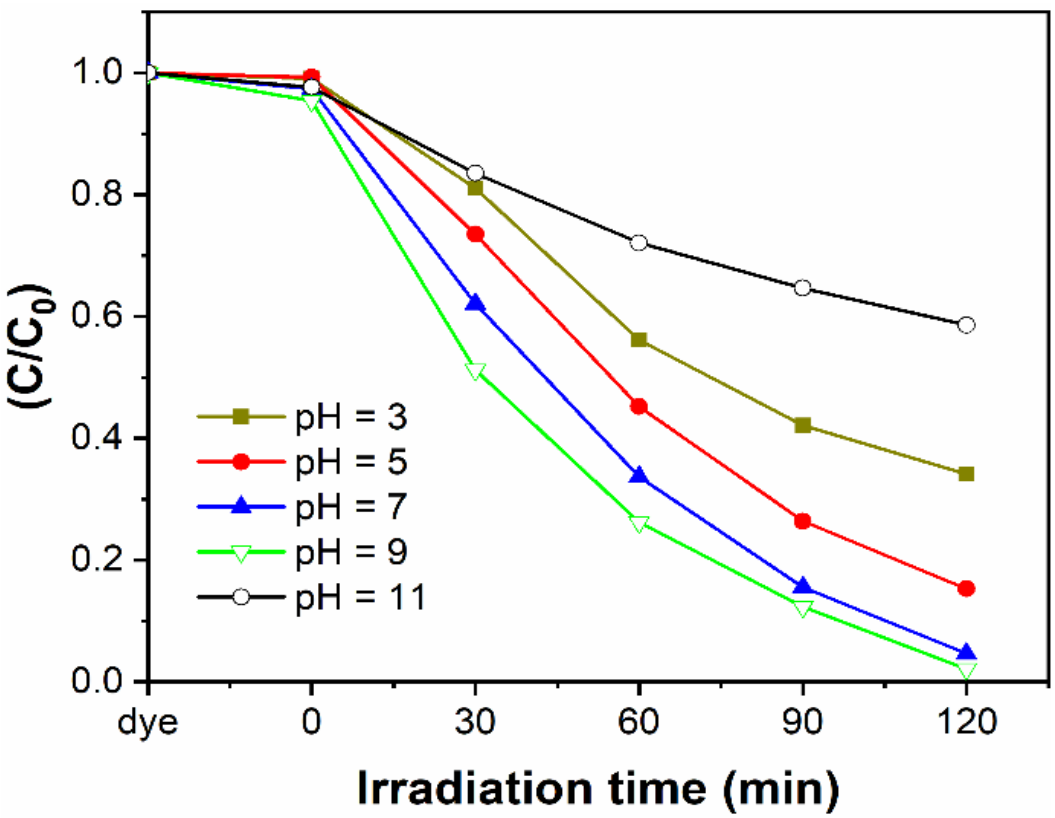

Fig. 6. Photodegradation of MB solution using 0.03 g of YFTO nanoparticles in different pH conditions.

surface of the photocatalyst, it is clear that the pH of solution has the significant effect on the photocatalytic efficiency [28]. Fig. 6 shows the photocatalytic efficiency of the YFTO in different pH conditions of the MB solution (3, 5, 7, 9, and 11). As can be seen, the degradation level of the MB solution in alkaline conditions (97.83% at pH = 9) is higher than that of in the acidic conditions (84.7% at pH = 5). These observations are attributed to the increased adsorption of MB molecules on the surface of YFTO photocatalyst in alkaline media. Due to the cationic characteristic of MB [29], there is the increased affinity to adsorb on the negatively surface charged of YFTO and in the higher pH values. However, more alkaline condition (pH = 11) led to the significant decrease in the photocatalytic degradation.

Reusability experiments

Reusability tests were carried out over 5 consecutive reaction cycles to evaluate the stability of the synthesized YFTO photocatalyst. After reaction cycle, the photocatalyst was separated by a bar magnet, washed several times with ethanol/deionized water solution. Then, the rinsed photocatalyst was dried at 90 °C for 1 h. Fig. 7 exhibits the performance of the MB photo-oxidation using 0.03 g of the YFTO photocatalyst over 5 reaction cycles. As seen, the decline in the photocatalytic efficiency is insignificant during 600 min of the consecutive reaction cycles (5 reactions), confirming superior stability of the YFTO photocatalyst. The loss of the photoactivity was only 2.85% after the fifth photodegradation reaction.

Additionally, Fig. 8 represents the XRD patterns for the YFTO photocatalyst before and after performing 5 successive experiments. There are no prominent changes in the crystalline structure, which validate the structural stability of the YFTO.

Photodegradation mechanism

In order to investigate the mechanism of the MB degradation using the YFTO photocatalyst, the radical scavenging experiments were carried out using varied radical scavengers. Eethylenediaminetetraacetic acid (EDTA) [30], ascorbic acid [31], and isopropanol were used to suppress the photogenerated holes, superoxide radicals, and hydroxyl radicals, respectively

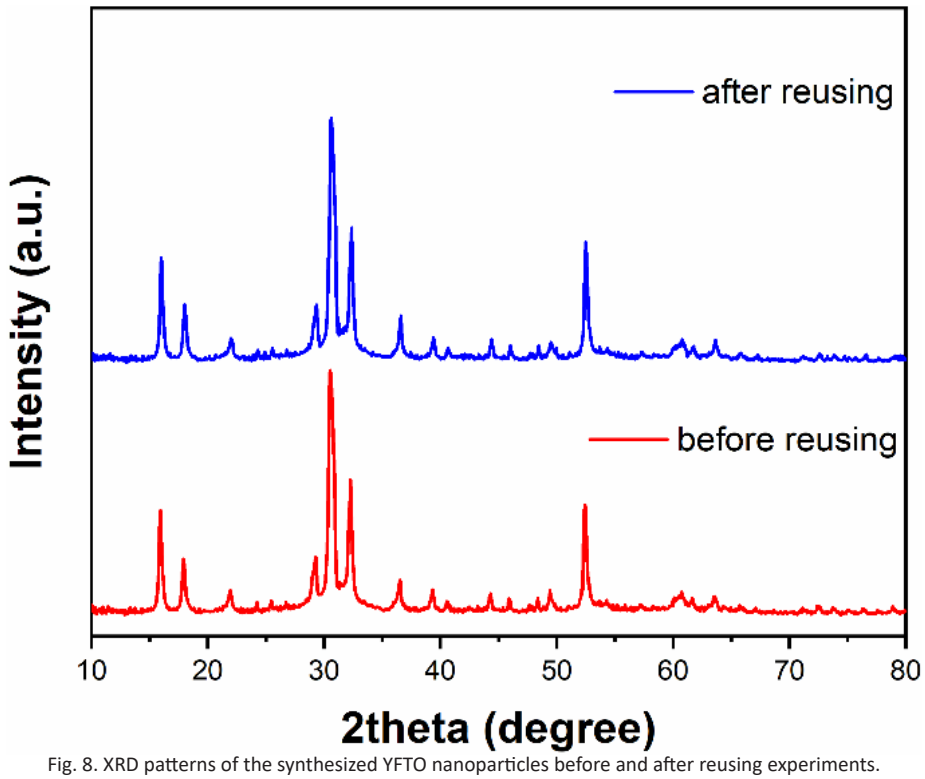

Fig. 8. XRD patterns of the synthesized YFTO nanoparticles before and after reusing experiments.

[32]. Fig. 9 exhibits the effect of different radical scavengers on the visible-light degradation of MB solution using the YFTO photocatalyst. As can be seen form the Fig. 9, the degradation level is significantly decreased in the presence of isopropanol and ascorbic acid, confirming the role

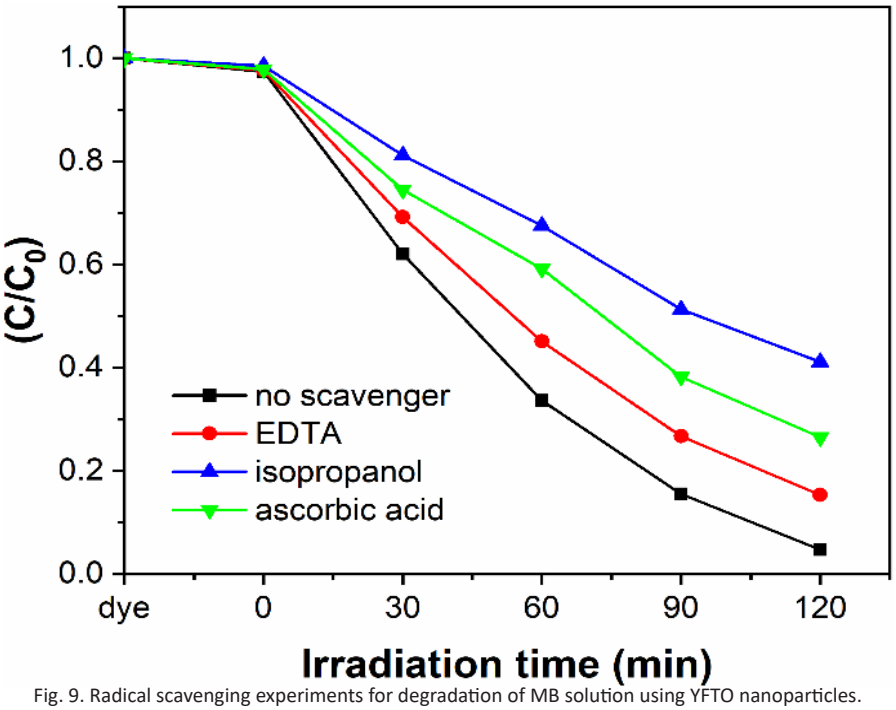

Fig. 9. Radical scavenging experiments for degradation of MB solution using YFTO nanoparticles.

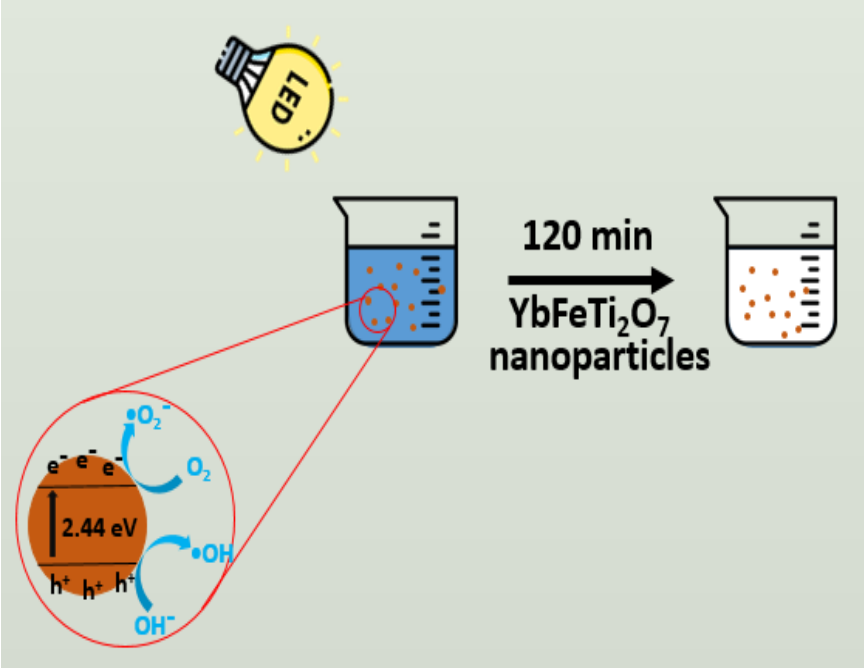

Fig. 10. Proposed mechanism for MB photodegradation using YFTO nanoparticles.

of superoxide ($\bullet O_2^-$) and hydroxyl (•OH) radicals to contribute in the degradation of MB molecules.

Fig. 10 depicts the mechanism of MB degradation using the synthesized YFTO nanoparticles. The light brown color YFTO nanoparticles dispersed in MB solution are activated by visible light beams emitted from the LED lamp. The photo-generated electrons and holes contribute in the redox reactions to form the highly activated $\bullet O_2^-$ and •OH radicals. The radicals are capable degrading the MB molecules during 120 min illumination.

CONCLUSION

In summary, we have presented the sol-gel synthesis of $YbFeTi_2O_7$, YFTO, nanoparticles as the magnetically separable photocatalyst. The DRS analysis confirmed that the synthesized YFTO nanoparticles have capability serving as the highly efficient visible light photocatalyst. The band gap of the nanoparticles was calculated to be 2.44 eV. The YFTO nanoparticles exhibit the superparamagnetic behavior, making them viable magnetic photocatalyst, which is crucial for efficient recovery of the photocatalyst particles from the reaction media using a bar magnet. The visible light photocatalytic performance of the synthesized nanoparticles was investigated for degradation of aqueous solution of MB. Using 0.03 g of the YFTO photocatalyst, the photocatalytic efficiency was approximately 95% under 120 min of visible light illumination. In addition, pH of MB solution influenced the photoactivity of YFTO nanoparticles, so that alkaline condition was in the favor of achieving the higher photodegradation level of MB. The reusability experiments showed the conspicuous photocatalytic performance over 5 successive reaction cycles, revealing the great structural stability as confirmed by XRD patterns. The radical scavenging investigations were also performed to study the degradation mechanism. It was found that the MB photodegradation reaction proceeded through oxidation using $\bullet O_2^-$ and •OH radicals.

CONFLICT OF INTEREST

The authors declare that there is no conflict of interests regarding the publication of this manuscript.

REFERENCES

1. Mohadesi M, Sanavi Fard M, Shokri A. The application of modified nano-TiO_2 photocatalyst for wastewater treatment: A review. Int J Environ Anal Chem. 2022;104(11):2571-2592.
2. Khader EH, Muslim SA, Saady NMC, Ali NS, Salih IK, Mohammed TJ, et al. Recent advances in photocatalytic advanced oxidation processes for organic compound degradation: A review. Desalination and Water Treatment. 2024;318:100384.
3. Bopape DA, Ntsendwana B, Mabasa FD. Photocatalysis as a pre-discharge treatment to improve the effect of textile dyes on human health: A critical review. Heliyon. 2024;10(20):e39316.
4. Chung K-T, Stevens SE, Cerniglia CE. The Reduction of Azo Dyes by the Intestinal Microflora. Crit Rev Microbiol. 1992;18(3):175-190.
5. Carmen Z, Daniel S. Textile Organic Dyes – Characteristics, Polluting Effects and Separation/Elimination Procedures from Industrial Effluents – A Critical Overview. Organic Pollutants Ten Years After the Stockholm Convention - Environmental and Analytical Update: InTech; 2012.
6. Song C, Xiao L, Chen Y, Yang F, Meng H, Zhang W, et al. TiO_2-Based Catalysts with Various Structures for Photocatalytic Application: A Review. Catalysts. 2024;14(6):366.
7. Schneider J, Matsuoka M, Takeuchi M, Zhang J, Horiuchi Y, Anpo M, et al. Understanding TiO_2 Photocatalysis: Mechanisms and Materials. Chem Rev. 2014;114(19):9919-9986.
8. Daghrir R, Drogui P, Robert D. Modified TiO_2 for Environmental Photocatalytic Applications: A Review. Industrial and Engineering Chemistry Research. 2013;52(10):3581-3599.
9. Rahbar M, Behpour M. Fluorite type $La_2Pb_2O_7$ nanoparticles coated onto AgO as enhanced performance cathode active material for alkaline primary cell. J Power Sources. 2022;521:230887.
10. Li X, Aftab S, Liu H, Vikraman D, Hussain S, Al-Kahtani AA, et al. Enhancing electron transport through metal oxide adjustments in perovskite solar cells and their suitability for X-ray detection. Journal of Materials Chemistry A. 2024;12(33):22310-22324.
11. Janani FZ, Khiar H, Taoufik N, Elhalil A, Sadiq M, Puga AV, et al. ZnO–Al_2O_3–CeO_2–Ce_2O_3 mixed metal oxides as a promising photocatalyst for methyl orange photocatalytic degradation. Materials Today Chemistry. 2021;21:100495.
12. Robert D. Photosensitization of TiO_2 by M_xO_y and M_xS_y nanoparticles for heterogeneous photocatalysis applications. Catal Today. 2007;122(1-2):20-26.
13. Abed SH, Shamkhi AF, Heydaryan K, Mohammadalizadeh M, Sajadi SM. Sol-gel Pechini preparation of $CuEr_2TiO_6$ nanoparticles as highly efficient photocatalyst for visible light degradation of acid red 88. Ceram Int. 2024;50(13):24096-24102.
14. Naeinian N, Imani M, Tadjarodi A. Mechanochemical synthesis of $CoFe_2O_4$/Bi_2MoO_6 mixed metal oxide and study of its photocatalytic behavior. Mater Lett. 2024;355:135512.
15. AlMohamadi H, Awad SA, Sharma AK, Fayzullaev N, Távara-Aponte A, Chiguala-Contreras L, et al. Photocatalytic Activity of Metal- and Non-Metal-Anchored ZnO and TiO_2 Nanocatalysts for Advanced Photocatalysis: Comparative Study. Catalysts. 2024;14(7):420.
16. Aoudjit L, Salazar H, Zioui D, Sebti A, Martins PM, Lanceros-Mendez S. Reusable Ag@TiO_2-Based Photocatalytic Nanocomposite Membranes for Solar Degradation of Contaminants of Emerging Concern. Polymers. 2021;13(21):3718.
17. Lee K-T, Lu S-Y. A cost-effective, stable, magnetically recyclable photocatalyst of ultra-high organic pollutant

degradation efficiency: $SnFe_2O_4$ nanocrystals from a carrier solvent assisted interfacial reaction process. Journal of Materials Chemistry A. 2015;3(23):12259-12267.
18. Rajabathar JR, Thankappan R, Sutha A, Al-Lohedan H, Mahmoud Karami A, Ashok Kumar S, et al. Enhanced photocatalytic activity of magnetite/titanate (Fe_3O_4/TiO_2) nanocomposite for methylene blue dye degradation under direct sunlight. Opt Mater. 2024;148:114820.
19. Vasiljević ZŽ, Dojčinović MP, Vujančević JD, Spreitzer M, Kovač J, Bartolić D, et al. Exploring the impact of calcination parameters on the crystal structure, morphology, and optical properties of electrospun Fe_2TiO_5 nanofibers. RSC Advances. 2021;11(51):32358-32368.
20. Nazeri M, Hosseinpour Mashkani SM, Chelongarian R. Synthesis of YTi@Ag nanocomposite and investigation of its structural and antifungal properties. Journal of the Iranian Chemical Society. 2019;17(1):103-110.
21. Peng K, Fu L, Yang H, Ouyang J. Perovskite $LaFeO_3$/ montmorillonite nanocomposites: synthesis, interface characteristics and enhanced photocatalytic activity. Sci Rep. 2016;6(1).
22. Thirumalairajan S, Girija K, Ganesh I, Mangalaraj D, Viswanathan C, Balamurugan A, et al. Controlled synthesis of perovskite $LaFeO_3$ microsphere composed of nanoparticles via self-assembly process and their associated photocatalytic activity. Chem Eng J. 2012;209:420-428.
23. Qiu W, Zheng Y, Haralampides K. Study on a novel POM-based magnetic photocatalyst: Photocatalytic degradation and magnetic separation. Chem Eng J. 2007;125(3):165-176.
24. Wells J, Kazakova O, Posth O, Steinhoff U, Petronis S, Bogart LK, et al. Standardisation of magnetic nanoparticles in liquid suspension. J Phys D: Appl Phys. 2017;50(38):383003.
25. Zhou X, Dong H. A Theoretical Perspective on Charge Separation and Transfer in Metal Oxide Photocatalysts for Water Splitting. ChemCatChem. 2019;11(16):3688-3715.
26. Huang W, Lu X, Jia D, Huang J, Li Z, Xie H, et al. Characterization of structural, optical and photocatalytic properties of yttrium modified hematite (α-Fe_2O_3) nanocatalyst. Ceram Int. 2023;49(15):25602-25611.
27. Moniz SJA, Shevlin SA, An X, Guo ZX, Tang J. Fe_2O_3–TiO_2 Nanocomposites for Enhanced Charge Separation and Photocatalytic Activity. Chemistry – A European Journal. 2014;20(47):15571-15579.
28. Kumar A. A Review on the Factors Affecting the Photocatalytic Degradation of Hazardous Materials. Material Science and Engineering International Journal. 2017;1(3).
29. Rahmani S, Zeynizadeh B, Karami S. Removal of cationic methylene blue dye using magnetic and anionic-cationic modified montmorillonite: kinetic, isotherm and thermodynamic studies. Applied Clay Science. 2020;184:105391.
30. Fu J, Tian Y, Chang B, Xi F, Dong X. BiOBr–carbon nitride heterojunctions: synthesis, enhanced activity and photocatalytic mechanism. J Mater Chem. 2012;22(39):21159.
31. Liang Y, Lin S, Liu L, Hu J, Cui W. Oil-in-water self-assembled Ag@AgCl QDs sensitized Bi_2WO_6: Enhanced photocatalytic degradation under visible light irradiation. Applied Catalysis B: Environmental. 2015;164:192-203.
32. Elahifard MR, Gholami MR. Acid blue 92 photocatalytic degradation in the presence of scavengers by two types photocatalyst. Environmental Progress and Sustainable Energy. 2011;31(3):371-378.